Archive of Applied Mechanics 73 (2003) 282 – 309 © Springer-Verlag 2003
DOI 10.1007/s00419-003-0292-7

Effective bending stiffness for plates with microcracks

D. C. Simkins Jr, S. Li

Summary In this paper, micromechanics methods are applied to characterize the damage of plate structures, both Love-Kirchhoff and Reissner-Mindlin plates, due to microcrack distribution. Analytical expressions for effective stiffness of a damaged plate with distributed microcracks are derived for the first time. The results are compared with the results based on continuum damage theory, and it is found that there are significant differences between the two. It is well known that constitutive relations at the structural level, e.g. curvature/moment relation, and shear/transverse strain relation, are fundamentally different from the constitutive relation at the material level, i.e. stress/strain relations. This is because a priori kinematic assumptions in engineering structural theories pose additional constitutive constraints on the relationships between stress resultant/couple and strain measures. The newly derived effective stiffness formulae for various plates reflect such constitutive constraints, and therefore are consistent with engineering plate theories. They provide an alternative means in structure designs and structure damage evaluations.

Keywords Microcracks, Damage, Fracture, Micromechanics, Kirchhoff plate, Reissner-Mindlin plate, Nanofilm, Representative plate element

1 Introduction

Plate-like structures have many engineering applications. They are primary structural components in aerospace, civil, and mechanical engineering. Mathematical plate theories, such as the classical (Kirchhoff) plate theory as well as the Reissner-Mindlin plate theory, are the corner stones of structural engineering. In the rest of the paper a Love-Kirchhoff plate is referred to as the thin plate, whereas a Reissner-Mindlin plate is referred to as the thick plate. By utilizing plate theories in designs, which capture the essential characters of plate-like structural deformations, engineers enjoy the advantage of reduced complexity of plate elements over three-dimensional (3D) continuum theory.

The basic difference between plate theories and 3D elasticity theory is that in the former theories a priori kinematic assumptions are introduced in order to filter out trivial deformation modes while retaining or emphasizing important deformation modes, such as bending and transverse shear modes. Mathematically speaking, the plate theory is a self-contained logic set, and can be viewed as an independent subject from 3D elasticity theory, though their derivation departs from 3D elasticity (not necessary) and their accuracy is referenced to 3D elasticity solutions. In most physics-based treatments, plate equilibrium equations are derived by integrating (averaging) through the plate thickness and determining stress resultants, while conforming with the kinematic assumptions. This procedure is literally a homogenization as well, but both its physical implication as well as objective

Received 13 May 2002; accepted for publication 17 April 2003

D. C. Simkins Jr, S. Li (✉)
Department of Civil and Environmental Engineering,
University of California, Berkeley, CA 94720, USA
e-mail: li@ce.berkeley.edu

The work is supported by an Junior Faculty Research Fund (BURNL-07427-11503-EGSLI) to Professor Shaofan Li provided by the senate committee on research of University of California at Berkeley. The authors would like to thank the referees of AAM helpful comments and suggestions.

are different from the homogenization in micromechanics. Finally, this procedure leads to new constitutive relations at the structural level. They are, in fact, the projection of constitutive relations of 3D continuum to a flat 2D manifold, in which the stress resultants are linked to strain measures at the structural level in terms of material elastic properties and the plate's geometry.

Due to the internal kinematic constraint, for both thin or thick plates, their constitutive relations at the structural level differ fundamentally from the elastic constitutive laws at the material level. This distinction has been long noted, and several writings have been devoted to this issue, e.g. [13–15].

Today, most plate structures are made of composite materials, e.g. [18, 19]. Recently, micromechanics and homogenization techniques have been employed to study inhomogeneous plates with microstructures, e.g. [9, 10, 11]. In fact, homogeneous plate is an idealization. In reality, there is no such thing as a homogeneous plate. Any plate component, whether homogeneous or not, will eventually degrade during loading service into an inhomogeneous state, because of the initiation as well as evolution of damage.

Questions of great practical importance are, how do these plate elements behave, to what extent can plate theories still be used when they are damaged by many microcracks (see Fig. 1), as may happen, e.g., as a result of an earthquake or blast loading. If plate theories can still be used after initial material damage or degradation, how can we use them in a correct fashion without compromising the relevant mathematical and physical principles, such as the kinematic assumptions.

Moreover, in the recent development of nanotechnolgy and micro-electro-mechanical systems (MEMS), primary miniature structural component in these technologies are thin plate-like films or a thin plate-like graphite sheets, which is the substance of a nanotube. The effective stiffnesses of these miniature plates are of great importance and concern in applications, because there are many microcracks embedded in these thin films or thin sheets. For instance, the main technical advantage of the nanotube is its ultra-strength, and the presence of microcracks will significantly reduce that strength. There have been a few experimental and numerical studies on the effect of microcracks on effective properties of thin films and nanotubes e.g. [21], [12], and [6], and nanotubes, [3], and [2]. However, there is still a lack of complete understanding of the subject.

At the macroscale, the effective material properties of a solid with randomly distributed microcracks can be evaluated by using standard micromechanics techniques, e.g. [7, 16]. For a plate member with randomly distributed microcracks, its effective stiffness has been evaluated according to the engineering "folklore" in the past, i.e. the effective elastic moduli obtained from continuum homogenization are substituted into the plate constitutive relations to estimate the effective stiffness of a damaged plate. Apparently, this procedure may not be justified for a nanometer-thin graphite sheet, or a micrometer-thin film, because these miniature plate structures have never been a part of a 3D continuum either in manufacture process or in their performance configurations. By using 3D continuum approach, one could face the danger by neglecting the free-surface effects on effective stiffness. In fact, there is a demand for justfication and verification why the material strength used in nanotubes is often close to theoretical material strength.

In this work, a new procedure is proposed. We apply micromechanics techniques directly to plate theories and derive effective bending stiffness based on a consistent theoretical framework. By doing so, we believe that the free-surface effects on effective stiffness can be captured. Here a notion of *representative plate element* (RPE) is used, which is similar to the concept of representative volume element (RVE) in continuum micromechanics. A detailed discussion on this concept may be found in [10, 11]. We assume that the microcrack distribution in an RPE is

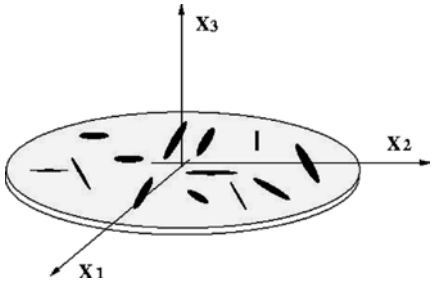

Fig. 1. A representative plate element with distributed microcracks

statistically stable, and the information on microcrack distribution density can be then linked as a damage index to assess the degradation of structure stiffness.

Based on this philosophy, the effective stiffness for both thin and thick damaged plates have been derived starting from the plate theories themselves in closed form. To assess the accuracy of this new method, the stiffnesses of damaged plates are examined in a comparison study. The arrangement of this paper is as follows: in Sec. 2, the basic formulas for both thin and thick plates are outlined. Some new averaging theorems in micromechanics of plate are proved. The main results for a cracked thin plate are presented in Sec. 3. The results for a cracked thick plate are presented in Sec. 4.

2
Formulations

For a self-contained treatment, formulations of thin and thick plates are outlined. Greek indices take on the values 1 and 2, and latin indices range from 1 to 3. For convenience, plate governing equations are presented in a scaled form. Let X_i be the real coordinates. Define

$$\epsilon := \begin{cases} \frac{h}{\sqrt{10}c}, & \text{for Reissner plate} \\ \frac{h}{\pi c}, & \text{for Mindlin plate} \end{cases},$$

$$x_i = \frac{X_i}{c},$$

where c is the half-length of the crack, and h is the plate thickness.

Since the objective of this work is the averaging of the analytic solution of a single crack in a plate, the departure point is fracture mechanics of plate theories. In Fig. 2, a plate with a penetrating crack in a general state of loading is illustrated. Because of linearity it can be viewed as the superposition of two states: a uniform deformation state and a crack perturbation state, as shown in Fig. 3.

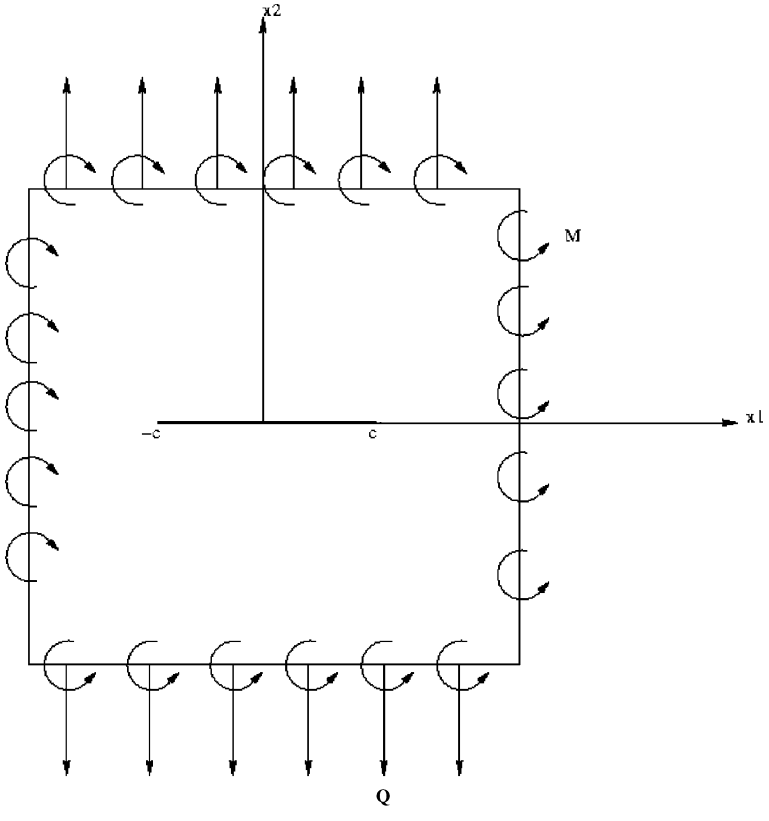

Fig. 2. Basic problem: a thin plate with single penetrating crack under general loading

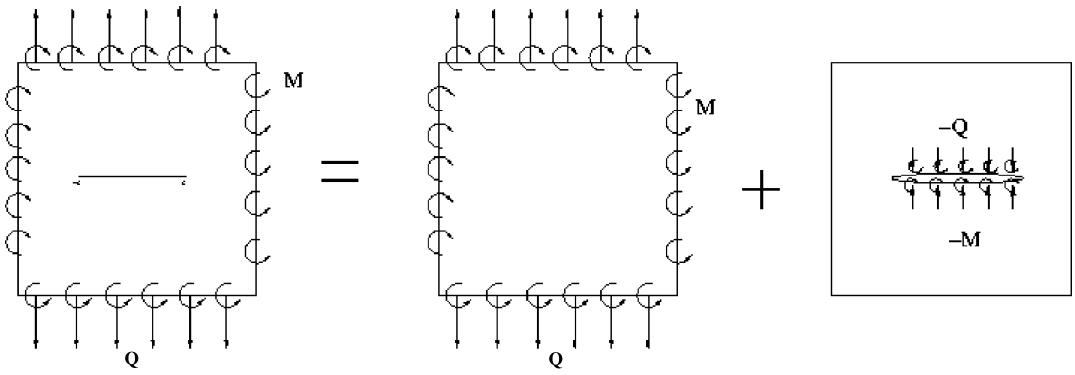

Fig. 3. Decomposing the basic problem into two sub-problems: uniform deformation and crack perturbation

2.1 Formulations for thin plates

The thin plate theory, also known as classical or Kirchhoff plate theory, neglects shear deformation, and requires that the fibers originally normal to the neutral surface remain normal. For isotropic plates, the classical plate equations in scaled coordinates are,

$$\beta_\mu = -\frac{1}{c} w_{,\mu} \ , \tag{1}$$

$$\kappa_{\mu\nu} = \frac{1}{2c}\left(\beta_{\mu,\nu} + \beta_{\nu,\mu}\right) \ , \tag{2}$$

$$\Delta\Delta w = \frac{c^4}{D} p \ , \tag{3}$$

$$M_{\mu\nu} = -\frac{D}{c^2}\left[(1-\nu) w_{,\mu\nu} + \nu\delta_{\mu\nu} w_{,\gamma\gamma}\right] \ , \tag{4}$$

$$Q_\mu = -\frac{D}{c^3}\frac{\partial}{\partial x_\mu}[\Delta w] \ . \tag{5}$$

where $\Delta := \partial_\mu\partial_\mu$ is the 2D Laplacian operator. For kinematic variables, w is the deflection, β_μ are rotations, and $\kappa_{\mu\nu}$ are curvatures; for force variables, $M_{\mu\nu}$ are moments, Q_μ are transverse shear resultant forces, and p is external pressure on the plate surface. The constant D is the plate rigidity, which is defined as

$$D := \frac{Eh^3}{12(1-\nu^2)} \tag{6}$$

in which E is the Young's modulus, and ν is the Poisson's ratio. Note that it is assumed that the vertical external load p has no influence on the thin plate stiffness. The external load p is always set to zero in the equilibrium equation in the RPE of a thin plate.

2.2 Formulations for thick plates

The thick plate, or Reissner-Mindlin plate, takes into account transverse shear deformation, but still requires that the fibers originally normal to the neutral plane remain straight. For isotropic thick plates, the kinematic and constitutive relations, as well as equilibrium equations are

$$\gamma_\mu = \beta_\mu + \frac{1}{c} w_{,\mu} \ , \tag{7}$$

$$\kappa_{\mu\nu} = \frac{1}{2c}\left(\beta_{\mu,\nu} + \beta_{\nu,\mu}\right) \ , \tag{8}$$

$$M_{\mu\nu} = \frac{D}{c}\left[(1-\nu)\beta_{\mu,\nu} + \nu\delta_{\mu\nu}\beta_{\gamma,\gamma}\right] \ , \tag{9}$$

$$Q_\mu = \frac{D(1-\nu)}{2c^2\epsilon^2}\left(\beta_\mu + \frac{1}{c}w_{,\mu}\right) \ , \tag{10}$$

$$M_{\mu\nu,\nu} - cQ_\mu = 0 \ , \tag{11}$$

$$\frac{1}{c}Q_{\mu,\mu} = -p \ , \tag{12}$$

where γ_μ are transverse shear strains. Note that again it is assumed that the vertical external load p has no influence on thick plate's stiffness, $p = 0$ in the equilibrium equation of a thick plate RPE.

2.3 Constitutive relations

The main objective of this paper is to evaluate constitutive relations of damaged members at the structural level, i.e. the constitutive relations relating the stress resultants, or stress couples, to the strain measures. It may be succinct to calculate the effective stiffness by using indicial notations. However, matrix notation is more convenient in practical applications. To serve both purposes, tensorial representations are presented so that the details of the calculation are apparent, and readily useable results for isotropic plates are presented in matrix form.

The relationship between the moments and curvatures, in matrix notation, are:

$$\begin{pmatrix} M_{11} \\ M_{22} \\ M_{12} \end{pmatrix} = D\begin{pmatrix} 1 & \nu & 0 \\ \nu & 1 & 0 \\ 0 & 0 & 1-\nu \end{pmatrix}\begin{pmatrix} \kappa_{11} \\ \kappa_{22} \\ \kappa_{12} \end{pmatrix} \ ,$$

$$\begin{pmatrix} \kappa_{11} \\ \kappa_{22} \\ \kappa_{12} \end{pmatrix} = \frac{1}{D(1-\nu^2)}\begin{pmatrix} 1 & -\nu & 0 \\ -\nu & 1 & 0 \\ 0 & 0 & 1+\nu \end{pmatrix}\begin{pmatrix} M_{11} \\ M_{22} \\ M_{12} \end{pmatrix} \ ,$$

$$\begin{pmatrix} Q_1 \\ Q_2 \end{pmatrix} = \frac{D(1-\nu)}{2}\begin{pmatrix} \gamma_1 \\ \gamma_2 \end{pmatrix} \ ,$$

In tensorial notation,

$$M_{\mu\nu} = L_{\mu\nu\zeta\eta}\kappa_{\zeta\eta} \ , \tag{13}$$

$$\kappa_{\mu\nu} = N_{\mu\nu\zeta\eta}M_{\zeta\eta} \ . \tag{14}$$

For isotropic plates, the elastic stiffnesses are

$$L_{\mu\nu\zeta\eta} = D(1-\nu)I_{\mu\nu\zeta\eta} + 2D\nu J_{\mu\nu\zeta\eta} \ . \tag{15}$$

In Eq. (15)

$$J_{\mu\nu\zeta\eta} := \frac{1}{2}\delta_{\mu\nu}\delta_{\zeta\eta} \ , \tag{16}$$

$$I_{\mu\nu\zeta\eta} := J_{\mu\nu\zeta\eta} + K_{\mu\nu\zeta\eta} \ , \tag{17}$$

and

$$K_{\mu\nu\zeta\eta} := \frac{1}{2}\left(\delta_{\mu\zeta}\delta_{\nu\eta} + \delta_{\mu\eta}\delta_{\nu\zeta} - \delta_{\mu\nu}\delta_{\zeta\eta}\right) \ , \tag{18}$$

where $\delta_{\alpha\beta}$ is Kronecker delta.

Define the fourth-order Cartesian tensor as

$$\mathbf{A} = A_{\alpha\beta\zeta\eta}\mathbf{e}_\alpha \otimes \mathbf{e}_\beta \otimes \mathbf{e}_\zeta \otimes \mathbf{e}_\eta \ .$$

The fourth-order tensors **J** and **K** with the components (16) and (18) have the following properties:

$$\mathbf{J} : \mathbf{J} = \mathbf{J} \ ,$$

$$\mathbf{J} : \mathbf{K} = \mathbf{0} \ ,$$

$$\mathbf{K} : \mathbf{K} = \mathbf{K} \ .$$

In terms of the **J**-**K** basis, the plate's stiffness as well as compliance tensors, **L** and **N**, can be written as

$$\mathbf{L} = \mathbf{D}\{(\mathbf{1} + \nu)\mathbf{J} + (\mathbf{1} - \nu)\mathbf{K}\} \ , \tag{19}$$

$$\mathbf{N} = \frac{\mathbf{1}}{\mathbf{D}}\left\{\frac{\mathbf{1}}{(\mathbf{1} + \nu)}\mathbf{J} + \frac{\mathbf{1}}{(\mathbf{1} - \nu)}\mathbf{K}\right\} \ . \tag{20}$$

Furthermore, for transverse shear deformation mode, the constitutive relation between transverse shear and transverse shear strain are

$$Q_\mu = G_{\mu\nu}\gamma_\nu \ , \tag{21}$$

$$\gamma_\mu = H_{\mu\nu}Q_\nu \ . \tag{22}$$

In the case of isotropic plates

$$G_{\mu\nu} = \frac{(1 - \nu)}{2} D\delta_{\mu\nu} \ . \tag{23}$$

2.4 Averaging theorems for plates

The micromechanics homogenization theory rests upon volume-averaging theorems. In this section, several averaging theorems in plate theories are proved. The averaging theorems for plate theories are similar to those of the continuum theory. We first show that prescribed remote deflection boundary condition leads to a link between average kinematic variables and the prescribed kinematic variables at remote boundary. We then show that for a plate with a crack, the average kinematic variable can be represented as the sum of the kinematic variable of a virgin plate plus an additional term due to the presence of crack if constant force or moment is applied on the remote boundary, which is referred to as the additional kinematic formula. To derive the additional term due to the presence of inhomogeneities, the Reciprocal Theorem in plate theories is needed in the analysis.

Before proceeding further, we first state the following well-known results.

Theorem 2.1 (Reciprocal Theorem for Plates)

1. *Suppose that there are two sets of self-equilibrating* (*loading/deflection*) *states,* $\{M^{(1)}_{\mu\nu}, w^{(1)}\}$ *and* $\{M^{(2)}_{\mu\nu}, w^{(2)}\}$ *for a thin plate. For any closed contour* ∂V *inside the thin plate, the following equality holds*

$$\int_{\partial V} M^{(1)}_{\mu\nu}\beta^{(2)}_\mu n_\nu \, \mathrm{d}S = \int_{\partial V} M^{(2)}_{\mu\nu}\beta^{(1)}_\mu n_\nu \, \mathrm{d}S \tag{24}$$

where

$$\beta_\mu^{(\alpha)} = -\frac{1}{c} w_{,\mu}^{(\alpha)} \ .$$

2. *Suppose that there are two sets of self-equilibrating states:* $\{M_{\mu\nu}^{(1)}, Q_\mu^{(1)}, \beta_\mu^{(1)}, w^{(1)}\}$ *and* $\{M_{\mu\nu}^{(2)}, Q_\mu^{(2)}, \beta_\mu^{(2)}, w^{(2)}\}$ *for a thick plate. For any closed contour* ∂V *inside the thick plate, the following equality holds*

$$\int_{\partial V} M_{\mu\nu}^{(1)} \beta_\mu^{(2)} n_\nu \, \mathrm{d}S + \int_{\partial V} Q_\mu^{(1)} w^{(2)} n_\mu \, \mathrm{d}S = \int_{\partial V} M_{\mu\nu}^{(2)} \beta_\mu^{(1)} n_\nu \, \mathrm{d}S + \int_{\partial V} Q_\mu^{(2)} w^{(1)} n_\mu \, \mathrm{d}S \tag{25}$$

The proof of the reciprocal theorems is standard (e.g [20] for thin plate), and is thus omitted here.

The next two results are for a thin plate.

Result 2.1
Suppose a thin plate is subjected to the prescribed deflection boundary condition

$$w = -\frac{c^2}{2} \kappa_{\mu\nu}^0 x_\mu x_\nu \ \forall \mathbf{x} \in \partial V \ .$$

The average curvature is equal to a prescribed constant $\langle \kappa_{\mu\nu} \rangle = \kappa_{\mu\nu}^0$.

Using the definition, and integration by parts,

$$\begin{aligned} \langle \kappa_{\mu\nu} \rangle :&= \frac{1}{V} \int_V \kappa_{\mu\nu} \, \mathrm{d}V = \frac{1}{2V} \int_V \left(\beta_{\mu,\nu} + \beta_{\nu,\mu} \right) \mathrm{d}V = -\frac{1}{2Vc} \left\{ \int_{\partial V} w_{,\mu} \, n_\nu \, \mathrm{d}S + \int_{\partial V} w_{,\nu} \, n_\mu \, \mathrm{d}S \right\} \\ &= -\frac{1}{V} \int_{\partial V} \kappa_{\mu\zeta}^0 x_\zeta n_\nu \, \mathrm{d}S = \frac{1}{V} \kappa_{\mu\zeta}^0 \int_{\partial V} x_\zeta n_\nu \, \mathrm{d}S \\ &= \kappa_{\mu\zeta}^0 \delta_{\zeta\nu} = \kappa_{\mu\nu}^0 \end{aligned}$$

Result 2.2
Suppose a thin plate with a single microcrack is subjected to the constant bending moment boundary conditions

$$M_{\mu\nu} = M_{\mu\nu}^0 \ \forall \mathbf{x} \in \partial V \ .$$

Then the average curvature is given by

$$\langle \kappa_{\mu\nu} \rangle = \kappa_{\mu\nu}^0 + \kappa_{\mu\nu}^c \ , \tag{26}$$

where

$$\kappa_{\mu\nu}^c := \frac{1}{2V} \int_{\partial\Omega} \left(\beta_\mu n_\nu + \beta_\nu n_\mu \right) \mathrm{d}S \ , \tag{27}$$

and $\kappa_{\mu\nu}^0 = N_{\mu\nu\zeta\eta} M_{\zeta\eta}^0$.

Let the remote boundary of the RPE be denoted by ∂V, the boundary of the crack be denoted by $\partial\Omega$.

Let us apply the following two loading conditions:

The first one is a uniform perturbation field, which may be thought of as being generated by a prescribed rotation field $\delta\boldsymbol{\beta} = \delta\boldsymbol{\kappa} \cdot \mathbf{x}$ on the entire boundary of RPE,

$$\delta \mathbf{t}^1 = \begin{cases} \delta M_{\mu\nu} n_\mu \mathbf{e}_\nu, & \forall \mathbf{x} \in \partial V \ , \\ -\delta M_{\mu\nu} n_\mu \mathbf{e}_\nu, & \forall \mathbf{x} \in \partial\Omega \ . \end{cases} \tag{28}$$

Result (2.1) asserts that $\langle \boldsymbol{\kappa}^1 \rangle = \delta\boldsymbol{\kappa}$. Since interior to the crack the RPE is homogeneous, it is plausible that

$$\boldsymbol{\kappa}^1 = \langle \boldsymbol{\kappa}^1 \rangle = \delta\boldsymbol{\kappa} \rightarrow \mathbf{M}^1 = \delta\mathbf{M} = \mathbf{L} : \delta\boldsymbol{\kappa} \ .$$

The second is the real field generated by the true boundary condition of the cracked plate

$$\mathbf{t}^2 = \begin{cases} M^0_{\mu\nu} n_\mu \mathbf{e}_\nu, & \forall\, \mathbf{x} \in \partial V \ , \\ 0, & \forall\, \mathbf{x} \in \partial\Omega \ . \end{cases} \tag{29}$$

Thereby, the corresponding fields become

$$\left(\mathbf{M}^1, \boldsymbol{\kappa}^1, \boldsymbol{\beta}^1\right) \rightarrow (\boldsymbol{\delta}\mathbf{M}, \delta\boldsymbol{\kappa}, \delta\boldsymbol{\beta} = \delta\boldsymbol{\kappa} \cdot \mathbf{x}) \ ,$$

and

$$\left(\mathbf{M}^2, \boldsymbol{\kappa}^2, \boldsymbol{\beta}^2\right) \rightarrow (\mathbf{M}, \boldsymbol{\kappa}, \boldsymbol{\beta}) \ .$$

Applying the Reciprocal Theorem Eq. (24) yields

$$\frac{1}{V}\int\limits_{\partial V} \delta M_{\mu\nu} n_\mu \beta_\nu \, \mathrm{d}S - \frac{1}{V}\int\limits_{\partial\Omega} \delta M_{\mu\nu} n_\mu \beta_\nu \, \mathrm{d}\Omega = \frac{1}{V}\int\limits_{\partial V} M^0_{\mu\nu} n_\mu \delta\beta_\nu \, \mathrm{d}S \ ,$$

and

$$\frac{1}{V}\int\limits_{\partial V} \delta M_{\mu\nu} n_\mu \beta_\nu \, \mathrm{d}S - \frac{1}{V}\int\limits_{\partial\Omega} \delta M_{\mu\nu} n_\mu \beta_\nu \, \mathrm{d}\Omega = \frac{1}{V}\int\limits_{\partial V} M^0_{\mu\nu} n_\mu \delta\kappa_{\gamma\nu} x_\gamma \, \mathrm{d}S \ .$$

Rearranging and using the constitutive relations, we get

$$\delta M_{\mu\nu}\left\{\frac{1}{V}\int\limits_{\partial V} n_\mu \beta_\nu \, \mathrm{d}S - \frac{1}{V}\int\limits_{\partial\Omega} n_\mu \beta_\nu \, \mathrm{d}\Omega - \frac{1}{V}\int\limits_{\partial V} M^0_{\zeta\eta} n_\zeta N_{\eta\gamma\mu\nu} \, x_\gamma \, \mathrm{d}S\right\} = 0 \ .$$

Since the virtual moment tensor is symmetric, the symmetric part of the expression in brackets must be zero, i.e.

$$\frac{1}{2V}\int\limits_{\partial V} \left(n_\mu \beta_\nu + n_\nu \beta_\mu\right) \mathrm{d}S = \frac{1}{2V}\int\limits_{\partial\Omega} \left(n_\mu \beta_\nu + n_\nu \beta_\mu\right) \mathrm{d}\Omega + \frac{M^0_{\zeta\eta} N_{\eta\gamma\mu\nu}}{V}\int\limits_{\partial V} n_\zeta \, x_\gamma \, \mathrm{d}S \ . \tag{30}$$

Since by definition

$$\kappa^0_{\mu\nu} = N_{\eta\zeta\mu\nu} M^0_{\zeta\eta} \ ,$$

and the first integral in (30) is $\langle \kappa_{\mu\nu} \rangle$, we obtain the desired result

$$\langle \kappa_{\mu\nu} \rangle = \kappa^0_{\mu\nu} + \kappa^c_{\mu\nu}$$

and

$$\kappa^c_{\mu\nu} = \frac{1}{2V}\int\limits_{\partial\Omega} \left(\beta_\mu n_\nu + \beta_\nu n_\mu\right) \mathrm{d}S \ . \tag{31}$$

We now provide analogous results for thick plates.

Result 2.3
Suppose a thick plate is subjected to rotation boundary condition

$$\beta_\mu = c\kappa^0_{\mu\nu} x_\nu \ \forall \mathbf{x} \in \partial V \ .$$

Then,

$$\langle \kappa_{\mu\nu} \rangle = \kappa^0_{\mu\nu} \ .$$

The proof is nearly identical to that in Result 2.1.

Result 2.4
Suppose a thick plate with a single microcrack is subjected to the constant bending moment boundary conditions

$$M_{\mu\nu} = M^0_{\mu\nu} \ \forall \mathbf{x} \in \partial V \ .$$

Then the average curvature is given by

$$\langle \kappa_{\mu\nu} \rangle = \kappa^0_{\mu\nu} + \kappa^c_{\mu\nu} \ ,$$

where

$$\kappa^c_{\mu\nu} = \frac{1}{2V} \int_{\partial\Omega} \left(\beta_\mu n_\nu + \beta_\nu n_\mu \right) \mathrm{d}S \ . \tag{32}$$

Noting that the applied shear force Q_μ on the boundary is zero, the result is trivially obtained by the same procedure as shown in Result 2.2.

To derive the averaging theorem for transverse shear strain, we consider a thick plate with an embedded single crack under a specific loading condition: a uniform transverse shear force, Q^0_μ, is applied at the remote boundary, and there is no applied transverse shear on the crack surfaces.

We then claim that:

Result 2.5
Suppose that a thick plate, V, with an embedded single crack is loaded at remote boundary, ∂V, by a constant shear force Q^0_μ, and equilibrating moment, $M_{\mu\nu}$, and there is no transverse shear acting on the crack surfaces, $\partial\Omega$. Then

$$\langle Q_\mu \rangle = Q^0_\mu \ . \tag{33}$$

Since $p = 0 \Rightarrow Q_{\mu,\mu} = 0, \ \forall \mathbf{x} \in V, \ Q_\mu = (Q_\nu x_\mu)_{,\nu}$. Therefore,

$$\begin{aligned}
\langle Q_\mu \rangle &= \frac{1}{V} \int_V Q_\mu \, \mathrm{d}V = \frac{1}{V} \int_V (Q_\nu x_\mu)_{,\nu} \, \mathrm{d}V \\
&= \frac{1}{V} \oint_{\partial V} Q_\nu x_\mu n_\nu \, \mathrm{d}S - \frac{1}{V} \oint_{\partial\Omega} Q_\nu x_\mu n_\nu \, \mathrm{d}S \\
&= \frac{1}{V} \oint_{\partial V} Q^{(0)}_\nu x_\mu n_\nu \, \mathrm{d}S \\
&= \frac{Q^0_\nu}{V} \int_V \delta_{\mu\nu} \, \mathrm{d}V = Q^0_\mu \ .
\end{aligned} \tag{34}$$

Note that the existence of an equilibrating moment on the boundary is essential. First, without additional moments, the transverse shear force alone may not ensure a global equilibrium state; second, the prescribed boundary moment can not be a uniform constant, which will lead to zero average transverse shear force (see [11]).

Result 2.6
Consider a thick plate RPE. At microlevel, it may be viewed as an infinitely thick plate with an embedded single crack, which is subjected to remote boundary conditions of constant shear forces Q^0_μ and associated equilibrating moment $M_{\mu\nu}$.

The average transverse shear strain is

$$\langle \gamma_\mu \rangle = \gamma^0_\mu + \gamma^c_\mu \ , \tag{35}$$

with

$$\gamma^c_\mu = \int_{\partial\Omega} w n_\mu \, \mathrm{d}S \ . \tag{36}$$

Consider the strain energy density $\bar{U}$ of the cracked plate

$$\bar{U} = \frac{1}{2} M^0_{\mu\nu} \kappa^0_{\mu\nu} + \frac{1}{2} Q^0_\mu \gamma^0_\mu - \frac{1}{V} \int_{\partial\Omega} Q^0_\mu w n_\mu \, \mathrm{d}S - \frac{1}{V} \int_{\partial\Omega} M^0_{\mu\nu} \beta_\mu n_\nu \, \mathrm{d}S \ ,$$

where the first two terms are the energy density for the undamaged plate, and the last two terms are energy release density for a single crack Ω. The complementary energy density is accordingly,

$$\begin{aligned} \bar{U}^c &= M^0_{\mu\nu} \kappa^0_{\mu\nu} + Q^0_\mu \gamma^0_\mu - \bar{U} \\ &= \frac{1}{2} M^0_{\mu\nu} \kappa^0_{\mu\nu} + \frac{1}{2} Q^0_\mu \gamma^0_\mu + \frac{1}{V} \int_{\partial\Omega} Q^0_\mu w n_\mu \, \mathrm{d}S + \frac{1}{V} \int_{\partial\Omega} M^0_{\mu\nu} \beta_\mu n_\nu \, \mathrm{d}S \ . \end{aligned} \tag{37}$$

Since the transverse shear force is constant at remote boundary and is zero at crack surfaces, by Result 2.5 we get:

$$\langle Q_\mu \rangle = Q^0_\mu \ . \tag{38}$$

Consequently, one can calculate the average shear strain by

$$\langle \gamma_\mu \rangle = \frac{\partial \bar{U}^c}{\partial \langle Q_\mu \rangle} = \frac{\partial \bar{U}^c}{\partial Q^0_\mu} \ . \tag{39}$$

Substituting (37) into (39) yields

$$\langle \gamma_\mu \rangle = \gamma^0_\mu + \gamma^c_\mu = \gamma^0_\mu + \frac{1}{V} \int_{\partial\Omega} w n_\mu \, \mathrm{d}S \ , \tag{40}$$

where $\gamma^0_\mu = H_{\mu\nu} Q^0_\nu$.

3
Effective bending stiffness for a thin plate with microcracks

The stiffness for a thin damaged plate is determined by using the additional curvature formula (27) for a thin plate loaded at infinity by uniform bending and twisting moments. The plate has no transverse shear load. With the additional curvature for a single crack, a standard averaging procedure, [17], is used to determine the moduli for a distribution of microcracks with random orientations. The uniform loads at infinity are consistent with the Representative Plate Element (RPE) concept.

3.1
Crack solutions for thin plates

The mode-I and mode-II crack problems in thin plate theory have been studied before, e.g. [18]. For convenience, the solution of a thin plate with a penetrating crack is reformulated in a

systematic fashion, and they are listed in Appendix A. The Crack Opening Curvature (COC) may be defined as an analogue to Crack Opening Displacement (COD) in fracture mechanics of linear elasticity, which can be used to estimate the magnitude of the additional strain as well as the porosity caused by microcrack distribution.

3.1.1
Pure bending load

From Appendix A, the resulting expressions for the rotations along the crack surface for a plate loaded with constant remote bending M_0 are

$$\beta_1(x_1,0) = \frac{M_0 c}{D}\frac{4}{(3+\nu)(1-\nu^2)}x_1 \ , \tag{41}$$

$$\beta_2(x_1,0) = \frac{2M_0 c}{D(3+\nu)(1-\nu)}\sqrt{1-x_1^2} \ . \tag{42}$$

Based on Result 2.2,

$$\kappa^c_{\mu\nu} = \frac{1}{2V}\int\limits_{\partial\Omega}\left(\beta_\mu n_\nu + \beta_\nu n_\mu\right)\mathrm{d}S = \frac{1}{2V}\int\limits_{\partial\Omega^+}\left(\left[\beta_\mu\right]n_\nu + [\beta_\nu]n_\mu\right)\mathrm{d}S \ ,$$

where $\left[\beta_\mu\right] = \beta^+_\mu - \beta^-_\mu$. For this crack, $n_1 = 0$ and $n_2 = 1$, so,

$$\begin{aligned}\kappa^c_{11} &= \kappa^c_{12} = 0 \ , \\ \kappa^c_{22} &= \frac{2\pi M_0 c^2}{VD(3+\nu)(1-\nu)} \ .\end{aligned} \tag{43}$$

3.1.2
Pure twist load

The resulting expressions for the rotations along crack surface of a plate loaded with constant remote twist H_0 are

$$\beta_1(x_1,0) = \frac{H_0 c(1+\nu)}{2D(1-\nu)}\sqrt{1-x_1^2} \ , \tag{44}$$

$$\beta_2(x_1,0) = 0 \ . \tag{45}$$

We find,

$$\begin{aligned}\kappa^c_{11} &= \kappa^c_{22} = 0 \ , \\ \kappa^c_{12} &= \frac{\pi H_0 c^2(1+\nu)}{4\,\mathrm{D}V(1-\nu)} \ ,\end{aligned} \tag{46}$$

3.2
Averaging of aligned non-interacting microcracks

In this section, we compute the effective stiffness for a thin plate with a set of aligned cracks. We seek relationships of the form Eq. (4) and (5), replacing D with $\bar{D}$.

Following [17], define the crack density parameter, f. Assume that there are N_α microcracks in an RPE with crack length $2c_\alpha$. We further assume all cracks are oriented parallel to the x_1 axis.

Define crack density parameter for a particular crack length,

$$f_\alpha := \frac{N_\alpha c_\alpha^2}{V} \ , \tag{47}$$

and the overall density parameter,

$$f := \sum_{\alpha=1}^{n} f_\alpha \ . \tag{48}$$

The compliance tensor for a damaged plate can be written:

$$\bar{\mathbf{N}} = \mathbf{N} + \mathbf{H} \tag{49}$$

where $\mathbf{N}$ is the compliance of the undamaged plate and $\mathbf{H}$ is the change due to the cracks.

Thus,

$$\boldsymbol{\kappa}^c = \mathbf{H} : \mathbf{M} \ , \tag{50}$$

and we can determine the components of $\mathbf{H}$ directly from the results in the previous sections for a set of non-interacting cracks.

The matrix form of Eq. (50) is

$$\begin{bmatrix} \kappa_{11}^c \\ \kappa_{22}^c \\ \kappa_{12}^c \end{bmatrix} = \frac{f\pi}{D} \begin{bmatrix} 0 & 0 & 0 \\ 0 & \dfrac{2}{(3+\nu)(1-\nu)} & 0 \\ 0 & 0 & \dfrac{(1+\nu)}{4(1-\nu)} \end{bmatrix} \begin{bmatrix} M_0 \\ M_0 \\ H_0 \end{bmatrix} \ . \tag{51}$$

3.3
Averaging of randomly oriented and non-interacting microcracks

We now extend the results for the aligned microcracks to that for a uniform distribution of randomly oriented cracks, again assuming no interaction between cracks.

Denote with the superscript α the set of cracks with length c^α and oriented at an angle θ_α with respect to the x_1 axis. The non-zero components of $\mathbf{H}^\alpha$ can be found from Eq. (50):

$$\hat{H}^\alpha_{2222} = \frac{1}{D}\frac{2\pi}{(3+\nu)(1-\nu)} \ , \tag{52}$$

$$\hat{H}^\alpha_{1212} = \hat{H}^\alpha_{1221} = \hat{H}^\alpha_{2112} = \hat{H}^\alpha_{2121} = \frac{1}{D}\frac{\pi(1+\nu)}{8(1-\nu)} \ . \tag{53}$$

The transformation from $\mathbf{H}^\alpha$ to $\mathbf{H}$ is accomplished through the rotation tensor:

$$\mathbf{Q}^\alpha = \mathbf{e}^\alpha_\mu \otimes \mathbf{e}_\mu, \quad Q^\alpha_{\mu\nu} Q^\alpha_{\eta\nu} = \delta_{\mu\eta} \ . \tag{54}$$

We assume the cracks have density parameter f, thus we only need to average over orientation, crack length distribution is contained in f. To obtain $\mathbf{H}$, we write $\mathbf{H}^\alpha$ in the $\mathbf{H}$ basis, and integrate.

$$\begin{aligned} \mathbf{H} &= H_{\mu\nu\zeta\eta}\mathbf{e}_\mu \otimes \mathbf{e}_\nu \otimes \mathbf{e}_\zeta \otimes \mathbf{e}_\eta = \frac{f}{2\pi}\int_0^{2\pi} H^\alpha_{\mu\nu\zeta\eta}\mathbf{e}^\alpha_\mu \otimes \mathbf{e}^\alpha_\nu \otimes \mathbf{e}^\alpha_\zeta \otimes \mathbf{e}^\alpha_\eta \, \mathrm{d}\theta_\alpha \\ &= \left\{ \frac{f}{2\pi}\int_0^{2\pi} H^\alpha_{\xi\rho\sigma\tau} Q^\alpha_{\mu\xi} Q^\alpha_{\nu\rho} Q^\alpha_{\zeta\sigma} Q^\alpha_{\eta\tau} \, \mathrm{d}\theta_\alpha \right\} \mathbf{e}_\mu \otimes \mathbf{e}_\nu \otimes \mathbf{e}_\zeta \otimes \mathbf{e}_\eta \ . \end{aligned}$$

Since the orientations are random, $\mathbf{H}$ is an isotropic tensor, and can be written

$$H_{\mu\nu\zeta\eta} = h_1 \delta_{\mu\nu}\delta_{\zeta\eta} + \frac{1}{2}h_2\left(\delta_{\mu\zeta}\delta_{\nu\eta} + \delta_{\mu\eta}\delta_{\nu\zeta}\right) \ .$$

We can determine h_1 and h_2 through the use of Eq. (54) and Eqs. (52) and (53):

$$H_{\mu\mu\nu\nu} = 4h_1 + 2h_2 = f\hat{H}^{\alpha}_{\zeta\zeta\eta\eta} \ ,$$

$$H_{\mu\nu\mu\nu} = 2h_1 + 3h_2 = f\hat{H}^{\alpha}_{\zeta\eta\zeta\eta} \ .$$

Substituting, we get the following simultaneous equations:

$$4h_1 + 2h_2 = \frac{2\pi f}{D(3+\nu)(1-\nu)} \ ,$$

$$2h_1 + 3h_2 = \frac{f\pi}{2D}\frac{7+4\nu+\nu^2}{(3+\nu)(1-\nu)} \ .$$

Finally,

$$\mathbf{H} = \frac{\pi f}{D(3+\nu)(1-\nu)}\mathbf{J} + \frac{\pi f(7+4\nu+\nu^2)}{8D(3+\nu)(1-\nu)}\mathbf{K} \ . \tag{55}$$

Substituting Eq. (20) and Eq. (55) into Eq. (49) yields

$$\bar{\mathbf{N}} = \frac{1}{D}\left\{\left(\frac{1}{1+\nu} + \frac{\pi f}{(3+\nu)(1-\nu)}\right)\mathbf{J} + \left(\frac{1}{1-\nu} + \frac{\pi f(7+4\nu+\nu^2)}{8(3+\nu)(1-\nu)}\right)\mathbf{K}\right\} \ . \tag{56}$$

We now define $\bar{D}$ and $\bar{\nu}$ by

$$\bar{\mathbf{N}} = \frac{1}{\bar{D}}\left\{\frac{1}{1+\bar{\nu}}\mathbf{J} + \frac{1}{1-\bar{\nu}}\mathbf{K}\right\} \ . \tag{57}$$

Equating Eq. (57) and Eq. (56), we find

$$\frac{\bar{D}}{D} = \frac{1}{2}\left\{\frac{(3+\nu)(1-\nu^2)}{(3+\nu)(1-\nu)+\pi f(1+\nu)} + \frac{8(3+\nu)(1-\nu)}{8(3+\nu)+\pi f(7+4\nu+\nu^2)}\right\} \ , \tag{58}$$

and

$$\bar{\nu} = \frac{16\nu(3+\nu)+\pi f(1+\nu)(-1+4\nu+\nu^2)}{16(3+\nu)+\pi f(1+\nu)(15+4\nu+\nu^2)} \ . \tag{59}$$

3.4
Self-consistent estimate

Consider microcrack interaction. Self-consistent method [4, 5] is used to estimate effective stiffness matrix. It consists of solving Eq. (49), Eq. (20) and Eq. (55) simultaneously. In the solution process, virgin material properties D and ν are replaced by $\bar{D}$ and $\bar{\nu}$ in the last equation. Solving the implicit equation, we find,

$$\frac{\bar{D}}{D} = 2\left[\frac{(3+\bar{\nu})(1-\bar{\nu}^2)}{(3+\bar{\nu})(1-\bar{\nu})-\pi f(1+\bar{\nu})} + \frac{8(3+\bar{\nu})(1-\bar{\nu})}{8(3+\bar{\nu})-\pi f(7+4\bar{\nu}+\bar{\nu}^2)}\right]^{-1} \ . \tag{60}$$

To find the effective Poisson ratio, the roots to the following cubic must be computed:

$$\bar{\nu}^3 + a\bar{\nu}^2 + b\bar{\nu} + c = 0 \ ,$$

where

$$a = [-8(1+\lambda) + f\pi 5\lambda]\frac{1}{\lambda f\pi} \ ,$$

$$b = [-16(1+2\lambda) + f\pi(11\lambda - 8)]\frac{1}{\lambda f\pi} \ ,$$

$$c = [24(1-\lambda) + f\pi(7\lambda - 8)]\frac{1}{\lambda f \pi} \quad ,$$

$$\lambda := \frac{1-v}{1+v} \quad .$$

The analytic solution to this algebraic equation can be found in standard mathematics handbooks, e.g. [1],

$$q := \frac{1}{3}b - \frac{1}{9}a^2, \quad r := \frac{1}{6}(ab - 3c) - \frac{1}{27}a^3 \quad ,$$

$$s_1 := \sqrt[3]{r + \sqrt{q^3 + r^2}}, \quad s_2 := \sqrt[3]{r - \sqrt{q^3 + r^2}} \quad .$$

The roots are

$$\begin{aligned}
\bar{v}_1 &= (s_1 + s_2) - \frac{a}{3} \quad , \\
\bar{v}_2 &= -\frac{1}{2}(s_1 + s_2) - \frac{a}{3} + \frac{i\sqrt{3}}{2}(s_1 - s_2) \quad , \\
\bar{v}_3 &= -\frac{1}{2}(s_1 + s_2) - \frac{a}{3} - \frac{i\sqrt{3}}{2}(s_1 - s_2) \quad .
\end{aligned} \tag{61}$$

Only the last root, $\bar{v}_3$, satisfies the requirement

$$\lim_{f \to 0} \bar{v} = v$$

which is the physically meaningful solution.

3.5
Effective stiffness via continuum effective moduli

The effective flexibility $\bar{\mathbf{N}}$ can be computed by substituting effective material property values obtained in elastic continuum averaging, e.g. $\bar{E}$ and $\bar{v}$, into Eq. (6). The values for $\bar{E}$ and $\bar{v}$ for both the non-interacting and self-consistent method of effective matrix are available in [17]. These values are obtained from the corresponding averaging of a plane stress problem.

For the non-interacting distribution,

$$\frac{\bar{E}}{E} = \frac{1}{1 + \pi f} \quad , \tag{62}$$

$$\frac{\bar{v}}{v} = \frac{1}{1 + \pi f} \quad , \tag{63}$$

which lead to effective stiffness,

$$\frac{\bar{D}}{D} = \frac{(1 + \pi f)(1 - v^2)}{(1 + \pi f)^2 - v^2} \quad . \tag{64}$$

The effective material constants obtained from a self-consistent continuum averaging (plane stress problem) are

$$\frac{\bar{E}}{E} = 1 - \pi f \quad , \tag{65}$$

$$\frac{\bar{v}}{v} = 1 - \pi f \quad , \tag{66}$$

which lead to the effective stiffness for a thin plate

$$\frac{\bar{D}}{D} = \frac{(1-\pi f)(1-\nu^2)}{1-(1+\pi f)^2\nu^2} \quad . \tag{67}$$

These four results are compared in Fig. 4

From Fig. 4, one may find that the moduli obtained from plate averaging are much stiffer than the results obtained from continuum averaging. This implies that plate averaging provides a upper bound, whereas the continuum averaging may provide a lower bound for effective stiffness of a thin plate.

4
Effective stiffnesses of a thick plate with microcracks

Stiffnesses of a damaged thick plate are evaluated by using the averaging theorems presented in Sec. 2. These include both the bending stiffness and shear stiffness.

4.1
Crack solutions for thick plates

Crack solutions in a thick plate are presented in Appendix B. The thick plate is subjected to pure bending load, pure twist load and shear load.

4.1.1
Pure bending load

The resulting expressions for the rotations along the crack surface for a plate loaded with constant remote bending moment M_0 are

$$\beta_1(x_1, 0) = 0 \quad ,$$

$$\beta_2(x_1, 0) = \frac{2M_0 c}{D(1-\nu^2)}\sqrt{1-x_1^2} \quad ,$$

producing the COC's

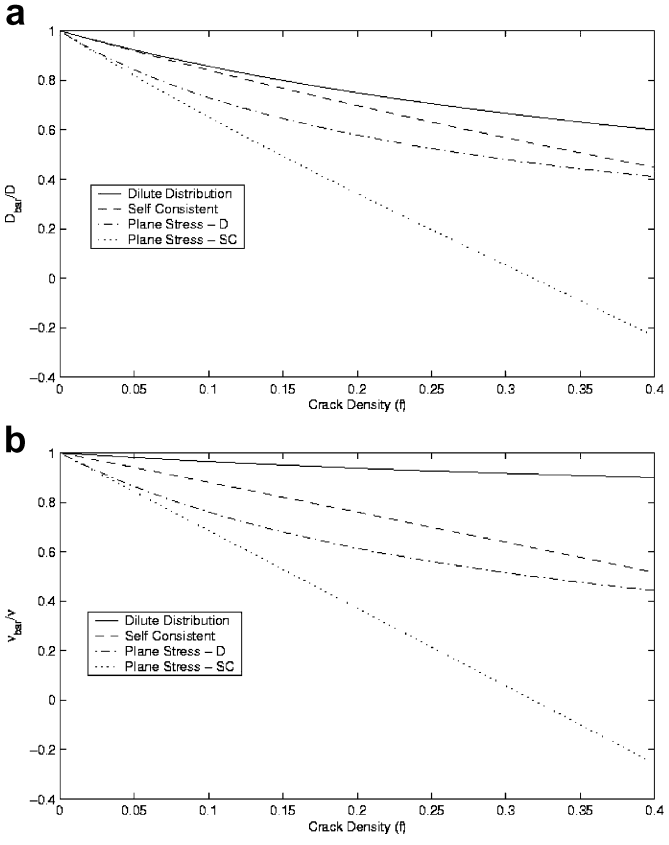

Fig. 4. Damaged stiffness for Kirchhoff-Love plates: **a**, **b**

$$\kappa_{11}^c = \kappa_{12}^c = 0 \ ,$$
$$\kappa_{22}^c = \frac{2M_0\pi c^2}{VD(1-\nu^2)} \ . \tag{68}$$

4.1.2
Pure twist load

The resulting expressions for the rotations of a plate loaded with constant remote twist H_0 along the crack surface are

$$\beta_1(x_1,0) = \frac{2H_0 c}{D(1-\nu^2)}\sqrt{1-x_1^2} \ ,$$
$$\beta_2(x_1,0) = 0 \ .$$

So, as before,

$$\kappa_{11}^c = \kappa_{22}^c = 0, \quad \text{and} \quad \kappa_{12}^c = \frac{\pi H_0 c^2}{VD(1-\nu^2)} \ . \tag{69}$$

4.1.3
Pure transverse shear load

To compute an effective shear modulus $\bar{G}$, we choose a plate with applied distributed shear along the top of the plate only. A distributed moment is also applied to satisfy equilibrium.

The results of the additional Crack Opening Shear Strain (COSS) are computed by using the displacement along the crack

$$w(x_1,0) = \frac{Q_0 c^3 \epsilon^2}{D(1-\nu)}\sqrt{1-{x_1}^2} \ ,$$

and Result 2.6 yields

$$\gamma_1^c = 0 \ , \tag{70}$$

$$\gamma_2^c = \frac{Q_0 c^4 \epsilon^2 \pi}{VD(1-\nu)} \ . \tag{71}$$

4.2
Averaging of aligned microcracks

In this section, we compute the effective stiffness of a thick plate following the methodology in Sec. 3.2. The quantities f, $\bar{\mathbf{N}}$, $\mathbf{H}$, and $\boldsymbol{\kappa}^c$ all have the same meaning as in Sec. 3.2. Using the results obtained in the previous section, we can find the individual components of $\mathbf{H}$ for the thick plate directly. In matrix form it is

$$\begin{bmatrix} \kappa_{11}^c \\ \kappa_{22}^c \\ \kappa_{12}^c \end{bmatrix} = \frac{f\pi}{D}\begin{bmatrix} 0 & 0 & 0 \\ 0 & \frac{2}{(1-\nu^2)} & 0 \\ 0 & 0 & \frac{1}{(1-\nu^2)} \end{bmatrix}\begin{bmatrix} M_0 \\ M_0 \\ H_0 \end{bmatrix} \ . \tag{72}$$

The total solution can then be written as

$$\begin{bmatrix} \kappa_{11} \\ \kappa_{22} \\ \kappa_{12} \end{bmatrix} = \frac{1}{D(1-\nu^2)}\begin{bmatrix} 1 & -\nu & 0 \\ -\nu & 1+2f\pi & 0 \\ 0 & 0 & 1+\nu+f\pi \end{bmatrix}\begin{bmatrix} M_0 \\ M_0 \\ H_0 \end{bmatrix} \ . \tag{73}$$

Similarly, for the shear modulus, we get

$$\gamma_2^c = H^0 \pi f Q_0, \quad \text{where } H^0 = \frac{2c^2\epsilon^2}{D(1-v)} \quad . \tag{74}$$

The total shear strains are

$$\begin{bmatrix} \gamma_1 \\ \gamma_2 \end{bmatrix} = \frac{2}{D(1-v)} \begin{bmatrix} 1 & 0 \\ 0 & 1 + \frac{\pi f h^2}{10} \end{bmatrix} \begin{bmatrix} Q_1 \\ Q_2 \end{bmatrix} \quad . \tag{75}$$

4.3
Averaging for randomly oriented and non-interacting microcracks

We now extend the results for the aligned microcracks to that for a uniform distribution of randomly oriented cracks, assuming no interaction between cracks. The non-zero components of **H** tensor in this case are

$$\hat{H}^{\alpha}_{2222} = \frac{2\pi}{D(1-v^2)} \quad \hat{H}^{\alpha}_{1212} = \hat{H}^{\alpha}_{1221} = \hat{H}^{\alpha}_{2112} = \hat{H}^{\alpha}_{2121} = \frac{\pi}{2D(1-v^2)} \quad . \tag{76}$$

The transformation from $\mathbf{H}^{\alpha}$ to **H** is accomplished as before, and **H** is found to be

$$\mathbf{H} = \frac{\pi f}{D(1-v^2)}\mathbf{J} + \frac{\pi f}{D(1-v^2)}\mathbf{K} \quad . \tag{77}$$

Substituting Eq. (20) and Eq. (77) into Eq. (49) yields

$$\bar{\mathbf{N}} = \frac{1}{D}\left\{ \left(\frac{1-v+\pi f}{1-v^2} \right)\mathbf{J} + \left(\frac{1+v+\pi f}{1-v^2} \right)\mathbf{K} \right\} \quad . \tag{78}$$

The final results are:

$$\frac{\bar{D}}{D} = \frac{(1-v^2)(1+\pi f)}{(1+\pi f)^2 - v^2} \quad , \tag{79}$$

and

$$\bar{v} = \frac{v}{1+\pi f} \quad . \tag{80}$$

It is interesting to note that the averaging results for thick plates appear to be the same as the 2D plane stress elasticity averaging solutions.

The matrix form now becomes

$$\begin{bmatrix} \kappa_{11} \\ \kappa_{22} \\ \kappa_{12} \end{bmatrix} = \frac{1}{D(1-v^2)} \begin{bmatrix} 1+f\pi & -v & 0 \\ -v & 1+f\pi & 0 \\ 0 & 0 & 1+v+f\pi \end{bmatrix} \begin{bmatrix} M_{11} \\ M_{22} \\ M_{12} \end{bmatrix} \quad . \tag{81}$$

Averaging over orientation for the shear modulus is only slightly more complicated. Unlike the bending case, this loading does depend on crack angle. Thus, the shear deformation at an angle α is $\gamma_{\alpha}^c = \gamma^c \cos\alpha$, and $H^{\alpha} = H^0 \cos\alpha$. Integrating α from 0 to 2π yields

$$H^c = H^0 \frac{\pi f}{2} \quad . \tag{82}$$

Finally, we obtain the effective shear stiffness,

$$\frac{\bar{G}}{G} = \left(\frac{\pi f}{2} \right)^{-1} \quad . \tag{83}$$

The averaged shear strains are

$$\begin{bmatrix} \gamma_1 \\ \gamma_2 \end{bmatrix} = \frac{2}{D(1-\nu)} \begin{bmatrix} 1+\frac{\pi f h^2}{20} & 0 \\ 0 & 1+\frac{\pi f h^2}{20} \end{bmatrix} \begin{bmatrix} Q_1 \\ Q_2 \end{bmatrix} \quad . \tag{84}$$

4.4 Self-consistent method

To take into account microcrack interaction, the self-consistent method [4, 5], is used to evaluate the effective stiffness of a thick plate. In fact, just like the case of non-interacting microcrack, the self-consistent estimates based on the thick plate theory yield the same results as the continuum self-consistent estimate (plane stress), Eqs. (66) and (67).

However for shear stiffness, the self-consistent method based on the thick theory provides a different answer

$$\frac{\bar{G}}{G} = 1 - \frac{\pi f}{2} \quad . \tag{85}$$

In Fig. 5, the effective stiffnesses computed from averaging of a thick plate in the cases of both dilute crack distribution as well as self-consistent method are displayed.

In Fig. 6, the effective shear stiffness computed from averaging of a thick plate in the cases of both dilute crack distribution as well as self-consistent method are juxtaposed with those computed based on continuum estimation.

5 Closure

In this work, a micromechanics averaging procedure is carried out to study the effective stiffness of damaged plates due to distributed microcracks. The novelty of this approach is that

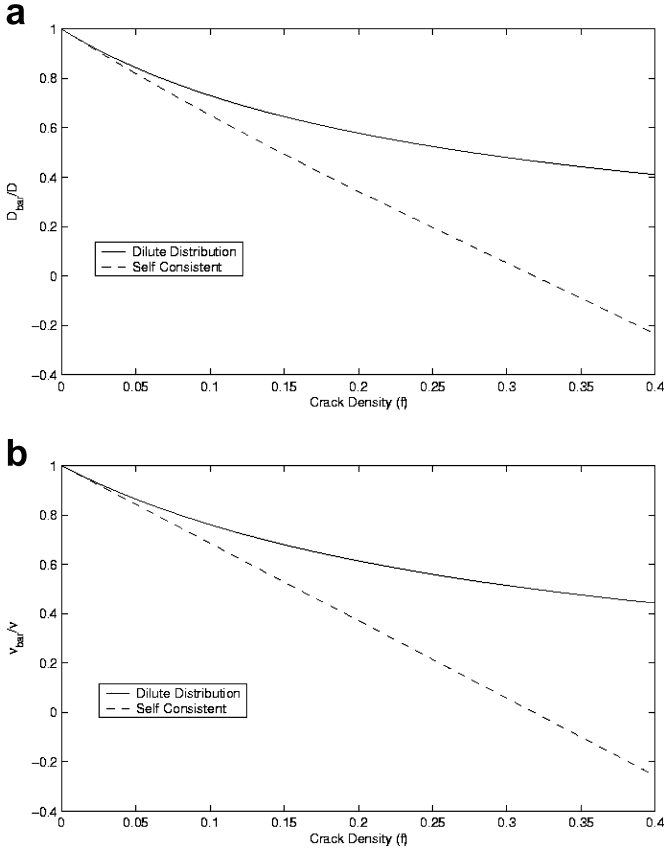

Fig. 5. Damaged stiffness for Reissiner-Mindlin plates: **a**, **b**

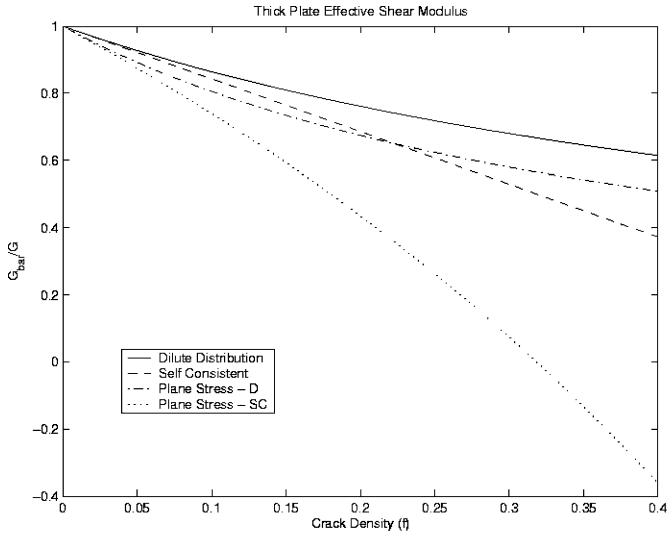

Fig. 6. Effective shear modulus for Reissiner-Mindlin plates

the averaging procedure is carried out within the framework of plate theories, which is in contrast to traditional procedure in which averaging is carried out at the material level. The results on effective stiffness of damaged plates, both thin plates and thick plates, based on these two different procedures are compared in different averaging schemes, such as non-interacting crack distribution as well as the self-consistent method of effective matrix. It is found that, in general, the stiffnesses derived from plate averaging theory are higher than those obtained based on plane stress elasticity averaging procedure for thin plates, but, perhaps surprisingly, yield exactly the same result for thick plate bending.

Apparently, it seems that the procedures proposed in this paper are only valid when crack length $2c$ is large in comparison to the plate thickness h, which may be unusual in the traditional civil engineering applications. Nevertheless, the applications under this scenario are both abundant and significant. This is especially true in the study of stiffness of a thin film or a nano-graphite sheet. In those circumstances, even a minute crack can have an enormous c/h ratio. An example of thick plate application may be randomly distributed faults, which usually have large c/h ratio comparing with the thickness of the earth crust.

It is interesting to note that in traditional averaging procedure the evaluation and homogenization of material damage proceed first in the continuum level, and constitutive projection procedure (integration through thickness) proceeds second, as if a material is degraded first, and one built a plate structure later by using the damaged material. Whereas, the new procedure proposed in this work implies a reversed order of the two procedures. As if one built a plate structure first by using a virgin material, and then evaluated the plate's damage, by homogenizing randomly distributed microcracks within structural theory. Obviously, in the second procedure, the damage theory as well as the micromechanics averaging theory are consistent with plate theories, i.e. the effective stiffness is derived directly based on plate theories providing a relationship that is consistent with the constraints imposed by the assumed kinematics.

Appendix A: Crack solutions for a thin plate

Since most crack solutions used in this work are not available in most literature, in this and the next Appendix, the crack solutions for both thin plate and thick plate are documented.

The thin plate has a single crack from $-c$ to c on the x_1-axis and is loaded on its boundary, assumed to be at infinity.

A.1. Solution for pure bending load

In this case, the plate is loaded at infinity by a uniform constant bending moment (in polar coordinates) $M_{rr} = M^0$. The boundary conditions are:

$$\lim_{r\to\infty}\begin{pmatrix} M_{rr} \\ M_{r\theta} \\ Q \end{pmatrix} = \begin{pmatrix} M_0 \\ 0 \\ 0 \end{pmatrix} \quad . \tag{A1}$$

Since the moments transform as second rank tensors, the following equations represent the boundary conditions:

$$M_{11}\cos^2\theta + M_{22}\sin^2\theta + 2M_{12}\sin\theta\cos\theta = M_0 \ ,$$

$$\frac{1}{2}(M_{22} - M_{11})\sin\theta\cos\theta + M_{12}\left(\cos^2\theta - \sin^2\theta\right) = 0 \ .$$

The crack problem has the following boundary conditions:

$$\lim_{x_2\to 0^+} M_{22}^c = -M_0 \quad \forall\,|x_1| < 1 \ , \tag{A2}$$

$$\lim_{x_2\to 0^+} \frac{\partial}{\partial x_2}\left(\frac{Dw^c}{c^2}\right) = 0 \quad \forall\,|x_1| > 1 \ , \tag{A3}$$

$$\lim_{x_2\to 0^+} Q_2^c + \frac{1}{c}M_{12,1}^c = 0 \quad \text{(Kirchhoff condition)} \ . \tag{A4}$$

Note that w is symmetric in both x_1 and x_2. We seek a solution of the following form:

$$\frac{Dw^c}{c^2} = \frac{1}{\pi}\int_0^\infty [A(\alpha)|x_2| + B(\alpha)]\mathrm{e}^{-\alpha|x_2|}\cos(\alpha x_1)\,\mathrm{d}\alpha.$$

By enforcing boundary condition (A4), we find that

$$B(\alpha) = -\frac{1+v}{\alpha(1-v)}A(\alpha) \ ,$$

$$\frac{Dw^c}{c^2} = \frac{1}{\pi}\int_0^\infty A(\alpha)\left(|x_2| - \frac{1+v}{\alpha(1-v)}\right)\mathrm{e}^{-\alpha|x_2|}\cos(\alpha x_1)\,\mathrm{d}\alpha \ .$$

Applying boundary conditions (A2) and (A3) yields the dual integral equations:

$$\frac{1}{\pi}\int_0^\infty A(\alpha)\cos(\alpha x_1)\,\mathrm{d}\alpha = 0 \quad \forall\,|x_1| > 1 \ ,$$

$$\frac{1}{\pi}\int_0^\infty \alpha A(\alpha)\cos(\alpha x_1)\,\mathrm{d}\alpha = -\frac{M_0}{3+v} \quad \forall\,|x_1| < 1 \ .$$

The solution of these equations is

$$A(\alpha) = -\frac{M_0}{3+v}\pi\frac{J_1(\alpha)}{\alpha} \ .$$

The solution for total deflection is

$$\frac{Dw}{c^2} = -\frac{M_0}{3+v}\int_0^\infty \frac{J_1(\alpha)}{\alpha}\left(|x_2| - \frac{1+v}{\alpha(1-v)}\right)\mathrm{e}^{-\alpha|x_2|}\cos(\alpha x_1)\ \mathrm{d}\alpha - \frac{M_0}{2(1+v)}\left({x_1}^2 + {x_2}^2\right) \ . \tag{A5}$$

Using this solution the rotations along x_1 are

$$\beta_1(x_1,0)=\begin{cases}\frac{M_0 c}{D}\frac{4}{(3+\nu)(1-\nu^2)}x_1, & |x_1|<1,\\ \frac{M_0 c(1+\nu)}{D(3+\nu)(1-\nu)\left(x_1+\sqrt{x_1^2-1}\right)}+\frac{M_0 c}{D(1+\nu)}x_1, & |x_1|>1\ ,\end{cases}$$

$$\beta_2(x_1,0)=\begin{cases}\frac{2M_0 c}{D(3+\nu)(1-\nu)}\sqrt{1-x_1^2}, & |x_1|<1,\\ 0, & |x_1|>1\ .\end{cases}$$

A.2. Solution for pure twist load

This case is similar to the pure bending case, but the remote loading is $M_{r\theta}=H_0=const.$

The boundary conditions are

$$\lim_{r\to\infty}\begin{pmatrix}M_{rr}\\ M_{r\theta}\\ Q\end{pmatrix}=\begin{pmatrix}0\\ H_0\\ 0\end{pmatrix}\ . \tag{A6}$$

The crack problem has the boundary conditions

$$\lim_{x_2\to 0^+}M_{12}^c=-H_0\quad\forall|x_1|<1\ , \tag{A7}$$

$$\lim_{x_2\to 0^+}\frac{Dw^c}{c^2}=0\quad\forall|x_1|>1\ . \tag{A8}$$

Note that this problem is anti-symmetric in both x_1 and x_2. By enforcing the anti-symmetry and Kirchhoff condition, we are seeking the solution of the following form:

$$\frac{Dw^c}{c^2}=\frac{\operatorname{sgn}x_2}{\pi}\int_0^\infty A(\alpha)\left(|x_2|-\frac{1+\nu}{\alpha(1-\nu)}\right)e^{-\alpha|x_2|}\sin(\alpha x_1)\,d\alpha\ .$$

Applying Eqs. (A7) and (A8), we get the dual integral equations

$$\frac{1}{\pi}\int_0^\infty \alpha A(\alpha)\cos(\alpha x_1)\,d\alpha=\frac{H_0}{2}\quad\forall|x_1|<1\ ,$$

$$\frac{1}{\pi}\int_0^\infty \frac{A(\alpha)}{\alpha}\sin(\alpha x_1)\,d\alpha=0\quad\forall|x_1|>1\ .$$

The solution to these equations is

$$A(\alpha)=\frac{\pi J_1(\alpha)}{\alpha}\frac{H_0}{2}\ .$$

The total solution then becomes

$$\frac{Dw}{c^2}=\frac{H_0}{2}\int_0^\infty\frac{J_1(\alpha)}{\alpha}\left(|x_2|-\frac{1+\nu}{\alpha(1-\nu)}\right)e^{-\alpha|x_2|}\sin(\alpha x_1)\,d\alpha-\frac{H^0}{1-\nu}x_1x_2\ .$$

The rotations along x_1 are

$$\beta_1(x_1,0) = \begin{cases} \frac{H_0 c(1+\nu)}{2D(1-\nu)}\sqrt{1-x_1^2} & |x_1|<1, \\ 0 & |x_1|>1 \ , \end{cases}$$

$$\beta_2(x_1,0) = -\frac{H_0 c}{D(1-\nu)}\left\{\int_0^\infty \frac{J_1(\alpha)}{\alpha}\cos(\alpha x_1)\,\mathrm{d}\alpha - x_1\right\} \ .$$

Finally,

$$\beta_2(x_1,0) = \begin{cases} 0 & |x_1|<1, \\ -\frac{H_0 c}{D(1-\nu)}\left[\frac{1}{x_1+\sqrt{x_1^2-1}} - x_1\right] & |x_1|>1 \ . \end{cases}$$

Appendix B: Crack solutions for a thick plate

In this Appendix, we provide the detailed derivation of crack solutions for a thick plate. The solutions presented here are modifications from references [8, 22–24].

The assumption that $p = 0$ in a thick plate RVE allows us to define a scalar potential function Φ from which the shear forces can be determined through

$$Q_1 = \frac{1}{c}\frac{\partial\Phi}{\partial x_2}, \quad Q_2 = -\frac{1}{c}\frac{\partial\Phi}{\partial x_1} \ . \tag{B1}$$

Combining these with Eqs (11) and (12), we obtain two equations in the two unknowns w and Φ:

$$\frac{\partial}{\partial x_2}\left[\Phi - \epsilon^2\Delta\Phi\right] + D\frac{\partial}{\partial x_1}\frac{\Delta w}{c^2} = 0 \ , \tag{B2}$$

$$\frac{\partial}{\partial x_1}\left[\Phi - \epsilon^2\Delta\Phi\right] - D\frac{\partial}{\partial x_2}\frac{\Delta w}{c^2} = 0 \ . \tag{B3}$$

These are the equations we solve for the bending and twist problems.

B.1. Solution for pure bending load

The loading is the same as for the thin plate case, with the same boundary conditions, Eq. (A1). The crack problem has the boundary conditions

$$\lim_{x_2\to 0^+}\begin{pmatrix} M_{22}^c \\ M_{12}^c \\ Q_2^c \end{pmatrix} = \begin{pmatrix} -M_0 \\ 0 \\ 0 \end{pmatrix} \quad \forall\,|x_1|<1 \ , \tag{B4}$$

and symmetry arguments dictating

$$\lim_{x_2\to 0^+}\begin{pmatrix} M_{12}^c \\ Q_2^c \end{pmatrix} = \begin{pmatrix} 0 \\ 0 \end{pmatrix} \quad \forall\,|x_1| \ , \tag{B5}$$

$$\lim_{x_2\to 0^+} w_{,2}^c = 0 \quad \forall\,|x_1|>1 \ . \tag{B6}$$

Again, w^c is symmetric in both x_1 and x_2, but Φ is anti-symmetric in x_1 and x_2. We seek solutions of the form

$$\frac{Dw^c}{c^2} = \frac{1}{\pi}\int_0^\infty A(\alpha)\left(|x_2| - \frac{(1+v)}{\alpha(1-v)}\right)\mathrm{e}^{-\alpha|x_2|}\cos(\alpha x_1)\,\mathrm{d}\alpha \ ,$$

$$\Phi = \frac{1}{\pi}\int_0^\infty 2\alpha A(\alpha)\left[\mathrm{e}^{-\alpha|x_2|} - \mathrm{e}^{-\kappa|x_2|}\right]\sin(\alpha x_1)\,\mathrm{d}\alpha \ .$$

For convenience, the general solutions are listed as follows:

$$M_{11} = M_0 + \frac{2M_0}{(1+v)\pi}\int_0^\infty \left\{\left[2\epsilon^2\alpha^2 + \frac{(1-v)}{2}(1-\alpha|x_2|)\right]\mathrm{e}^{-\alpha|x_2|} - 2\epsilon^2\alpha\kappa\mathrm{e}^{-\kappa|x_2|}\right\} \times \alpha\tilde{A}(\alpha)\cos(\alpha x_1)\,\mathrm{d}\alpha \ ,$$

$$M_{22} = M_0 - \frac{2M_0}{(1+v)\pi}\int_0^\infty \left\{\left[2\epsilon^2\alpha^2 + \frac{3+v}{2} - \frac{(1-v)}{2}\alpha|x_2|\right]\mathrm{e}^{-\alpha|x_2|} - 2\epsilon^2\alpha\kappa\mathrm{e}^{-\kappa|x_2|}\right\} \times \alpha\tilde{A}(\alpha)\cos(\alpha x_1)\,\mathrm{d}\alpha \ ,$$

$$M_{12} = -\frac{2M_0\operatorname{sgn} x_2}{(1+v)\pi}\int_0^\infty \left\{\left[\left(1+2\epsilon^2\alpha^2\right) - \frac{(1-v)}{2}\alpha|x_2|\right]\mathrm{e}^{-\alpha|x_2|} - \left(1+2\epsilon^2\alpha^2\right)\mathrm{e}^{-\kappa|x_2|}\right\} \times \alpha\tilde{A}(\alpha)\sin(\alpha x_1)\,\mathrm{d}\alpha \ .$$

$$\beta_1 = \frac{M_0 c}{D(1+v)}x_1 + \frac{2M_0 c}{D(1-v^2)\pi}\int_0^\infty \left\{\left[2\epsilon^2\alpha^2 + \frac{(1+v)}{2} - \frac{(1-v)}{2}\alpha|x_2|\right]\mathrm{e}^{-\alpha|x_2|} - 2\epsilon^2\alpha\kappa\mathrm{e}^{-\kappa|x_2|}\right\} \times \tilde{A}(\alpha)\sin(\alpha x_1)\,\mathrm{d}\alpha \ ,$$

$$\beta_2 = \frac{M_0 c}{D(1+v)}x_2 + \frac{2M_0 c}{D(1-v^2)\pi}\int_0^\infty \left\{\left[2\epsilon^2\alpha^2 + 1 - \frac{(1-v)}{2}\alpha|x_2|\right]\mathrm{e}^{-\alpha|x_2|} - 2\epsilon^2\alpha^2\mathrm{e}^{-\kappa|x_2|}\right\} \times \tilde{A}(\alpha)\cos(\alpha x_1)\,\mathrm{d}\alpha \ ,$$

$$Q_1 = \frac{2M_0}{(1+v)\pi}\int_0^\infty \left[\alpha\mathrm{e}^{-\alpha|x_2|} - \kappa\mathrm{e}^{-\kappa|x_2|}\right]\alpha\tilde{A}(\alpha)\sin(\alpha x_1)\,\mathrm{d}\alpha \ ,$$

$$Q_2 = \frac{2M_0}{(1+v)\pi}\int_0^\infty \left[\mathrm{e}^{-\alpha|x_2|} - \mathrm{e}^{-\kappa|x_2|}\right]\alpha^2\tilde{A}(\alpha)\cos(\alpha x_1)\,\mathrm{d}\alpha \ .$$

Applying the first of boundary condition (B4) and (B6) yields the dual integral equations:

$$\frac{1}{\pi}\int_0^\infty \tilde{A}(\alpha)\cos(\alpha x_1)\,\mathrm{d}\alpha = 0 \quad \forall\,|x_1| > 1 \ ,$$

$$\frac{1}{\pi}\int_0^\infty \frac{2}{1+v}\left(\frac{3+v}{2} + 2\epsilon^2\alpha(\alpha-\kappa)\right)\alpha\tilde{A}(\alpha)\cos(\alpha x_1)\,\mathrm{d}\alpha = 1 \quad \forall\,|x_1| < 1 \ .$$

Taking the thick plate limit as $\epsilon \to \infty$, we find

$$\frac{1}{\pi}\int_0^\infty \alpha\tilde{A}(\alpha)\cos(\alpha x_1)\,\mathrm{d}\alpha = 1 \quad \forall\,|x_1|<1 \ ,$$

$$\frac{1}{\pi}\int_0^\infty \tilde{A}(\alpha)\cos(\alpha x_1)\,\mathrm{d}\alpha = 0 \quad \forall\,|x_1|>1 \ .$$

The solution of these equations is

$$\tilde{A}(\alpha) = \pi\frac{J_1(\alpha)}{\alpha} \ .$$

The thick limit rotations then become,

$$\beta_1(x_1,0) = \begin{cases} 0 & |x_1|<1, \\ \frac{M_0 c}{D(1+\nu)}\left(x_1 - \frac{1}{x_1+\sqrt{x_1^2-1}}\right) & |x_1|>1 \ , \end{cases}$$

$$\beta_2(x_1,0) = \begin{cases} \frac{2M_0 c}{D(1-\nu^2)}\sqrt{1-x_1^2} & |x_1|<1, \\ 0 & |x_1|>1 \ . \end{cases}$$

B.2. Solution for pure twist load
The crack problem has the boundary conditions

$$\lim_{x_2\to 0^+}\begin{pmatrix} M_{22}^c \\ M_{12}^c \\ Q_2^c \end{pmatrix} = \begin{pmatrix} 0 \\ -H_0 \\ 0 \end{pmatrix} \quad \forall\,|x_1|<1 \ , \tag{B7}$$

and the symmetry condition requires that,

$$\lim_{x_2\to 0^+}\beta_1^c = 0 \qquad \lim_{x_2\to 0^+} w^c = 0 \ . \tag{B8}$$

The problem is completely anti-symmetric in x_1 and x_2. To remain consistent with classical plate theory, we require that the shear deformation computed via Eq. (5) to match the shear deformation computed via Eq. (B1). This yields the solutions of following forms:

$$\frac{Dw^c}{c^2} = \frac{\operatorname{sgn} x_2}{\pi}\int_0^\infty [B(\alpha)+|x_2|A(\alpha)]\mathrm{e}^{-\alpha|x_2|}\sin(\alpha x_1)\,\mathrm{d}\alpha \ ,$$

$$\Phi = \frac{1}{\pi}\int_0^\infty \left\{-2\alpha A(\alpha)\mathrm{e}^{-\alpha|x_2|} + \frac{1}{\epsilon^2\kappa}\left[\left(1+2\epsilon^2\alpha^2\right)A(\alpha) - \alpha\frac{(1-\nu)}{2}B(\alpha)\right]\mathrm{e}^{-\kappa|x_2|}\right\}\cos(\alpha x_1)\,\mathrm{d}\alpha \ .$$

The general solutions are

$$M_{11} = \frac{1}{\pi}\int_0^\infty \Big\{ \big[(-4\epsilon^2\alpha^2 + \alpha^2(1-\nu)|x_2| + 2\alpha\nu)A(\alpha) + \alpha^2(1-\nu)B(\alpha)\big]e^{-\alpha|x_2|} + 2\alpha$$
$$\times \left[\big(1+2\epsilon^2\alpha^2\big)A(\alpha) - \frac{(1-\nu)}{2}\alpha B(\alpha)\right]e^{-\kappa|x_2|}\Big\}\sin(\alpha x_1)\,d\alpha \ ,$$

$$M_{22} = \frac{1}{\pi}\int_0^\infty \Big\{ \big[(4\epsilon^2\alpha^2 - \alpha^2(1-\nu)|x_2| + 2\alpha\nu)A(\alpha) - \alpha^2(1-\nu)B(\alpha)\big]e^{-\alpha|x_2|} - 2\alpha$$
$$\times \left[\big(1+2\epsilon^2\alpha^2\big)A(\alpha) - \frac{(1-\nu)}{2}\alpha B(\alpha)\right]e^{-\kappa|x_2|}\Big\}\sin(\alpha x_1)\,d\alpha \ ,$$

$$M_{12} = \frac{1}{\pi}\int_0^\infty \Big\{ (1-\nu)\left[\left(-\alpha - \frac{4\epsilon^2\alpha^2}{(1-\nu)} + \alpha^2|x_2|\right)A(\alpha) + \alpha^2 B(\alpha)\right]e^{-\alpha|x_2|} + \frac{\kappa^2+\alpha^2}{\kappa}$$
$$\times \left[\big(1+2\epsilon^2\alpha^2\big)A(\alpha) - \frac{(1-\nu)}{2}\alpha B(\alpha)\right]e^{-\kappa|x_2|}\Big\}\cos(\alpha x_1)\,d\alpha \ ,$$

$$\beta_1 = \frac{1}{\pi}\frac{c}{D}\int_0^\infty \Big\{ \left[\left(\frac{4\epsilon^2\alpha^2}{(1-\nu)} - \alpha|x_2|\right)A(\alpha) - \alpha B(\alpha)\right]e^{-\alpha|x_2|} - \frac{2}{(1-\nu)}$$
$$\times \left[\big(1+2\epsilon^2\alpha^2\big)A(\alpha) - \frac{(1-\nu)}{2}\alpha B(\alpha)\right]e^{-\kappa|x_2|}\}\cos(\alpha x_1)\,d\alpha \ ,$$

$$\beta_2 = \frac{1}{\pi}\frac{c}{D}\int_0^\infty \Big\{ \left[\left(-\frac{4\epsilon^2\alpha^2}{(1-\nu)} - 1 + \alpha|x_2|\right)A(\alpha) + \alpha B(\alpha)\right]e^{-\alpha|x_2|} + \frac{2}{(1-\nu)}\frac{\alpha}{\kappa}$$
$$\times \left[\big(1+2\epsilon^2\alpha^2\big)A(\alpha) - \frac{(1-\nu)}{2}\alpha B(\alpha)\right]e^{-\kappa|x_2|}\}\sin(\alpha x_1)\,d\alpha \ ,$$

$$Q_1 = \frac{1}{\pi}\int_0^\infty \left\{ 2\alpha^2 A(\alpha)e^{-\alpha|x_2|} - \frac{1}{\epsilon^2}\left[\big(1+2\epsilon^2\alpha^2\big)A(\alpha) - \frac{(1-\nu)}{2}\alpha B(\alpha)\right]e^{-\kappa|x_2|}\right\}\cos(\alpha x_1)\,d\alpha \ ,$$

$$Q_2 = \frac{1}{\pi}\int_0^\infty \left\{ -2\alpha^2 A(\alpha)e^{-\alpha|x_2|} + \frac{\alpha}{\epsilon^2\kappa}\left[\big(1+2\epsilon^2\alpha^2\big)A(\alpha) - \frac{(1-\nu)}{2}\alpha B(\alpha)\right]e^{-\kappa|x_2|}\right\}\sin(\alpha x_1)\,d\alpha \ .$$

Finally, by taking the thick crack limit, $\epsilon \to \infty$, we can obtain the dual integral equations:

$$\frac{1}{\pi}\int_0^\infty \alpha A(\alpha)\cos(\alpha x_1)\,d\alpha = \frac{-H_0}{(1+\nu)} \quad \forall\,|x_1| < 1 \ ,$$

$$\frac{1}{\pi}\int_0^\infty A(\alpha)\cos(\alpha x_1)\,d\alpha = 0 \quad \forall\,|x_1| > 1 \ .$$

The solutions to these equations are

$$A(\alpha) = \pi\frac{-H_0 J_1(\alpha)}{\alpha(1+\nu)} \ ,$$

while the thick plate rotations are

$$\beta_1(x_1,0)=\begin{cases}\frac{2H_0c}{D(1-\nu^2)}\sqrt{1-x_1^2} & |x_1|<1,\\ 0 & |x_1|>1\ ,\end{cases}$$

$$\beta_2(x_1,0)=\begin{cases}0 & |x_1|<1,\\ \frac{H_0c}{D(1-\nu)}\left[x_1-\frac{1}{x_1+\sqrt{x_1^2-1}}\right] & |x_1|>1\ .\end{cases}$$

B.3 Solution for transverse shear load

The crack solutions in the case of pure shear loading are obtained by solving the following equations:

$$\Delta\beta_1-\frac{1}{\epsilon^2}\beta_1=\frac{\partial}{\partial x_1}\left[\frac{1+\nu}{1-\nu}\frac{\Delta w}{c}+\frac{1}{\epsilon^2}\frac{w}{c}\right]\ , \tag{B9}$$

$$\Delta\beta_2-\frac{1}{\epsilon^2}\beta_2=\frac{\partial}{\partial x_2}\left[\frac{1+\nu}{1-\nu}\frac{\Delta w}{c}+\frac{1}{\epsilon^2}\frac{w}{c}\right]\ . \tag{B10}$$

The general solutions are

$$\frac{Dw}{c^2}=\frac{2Q_0c}{(1-\nu^2)}\int_0^\infty\left[\frac{(1-\nu)}{2}|x_2|A(\alpha)+B(\alpha)\right]e^{-\alpha|x_2|}\cos(\alpha x_1)\,d\alpha\ ,$$

$$M_{11}=\frac{2Q_0c}{(1+\nu)}\int_0^\infty\left\{\left[\left(\frac{(1-\nu)}{2}\alpha^2|x_2|+\alpha\nu-2\alpha^2\epsilon^2\right)A(\alpha)+\alpha^2B(\alpha)\right]e^{-\alpha|x_2|}+\alpha C(\alpha)e^{-\kappa|x_2|}\right\}\times\cos(\alpha x_1)\,d\alpha\ ,$$

$$M_{22}=\frac{2Q_0c}{(1+\nu)}\int_0^\infty\left\{\left[\left(-\frac{(1-\nu)}{2}\alpha^2|x_2|+\alpha+2\alpha^2\epsilon^2\right)A(\alpha)-\alpha^2B(\alpha)\right]e^{-\alpha|x_2|}-\alpha C(\alpha)e^{-\kappa|x_2|}\right\}\times\cos(\alpha x_1)\,d\alpha\ ,$$

$$M_{12}=\frac{2Q_0c}{(1+\nu)}\int_0^\infty\left\{\left[\left(-\frac{(1-\nu)}{2}\alpha^2|x_2|+\frac{(1-\nu)}{2}\alpha+2\alpha^3\epsilon^2\right)A(\alpha)-\alpha^2B(\alpha)\right]e^{-\alpha|x_2|}-\frac{\kappa^2+\alpha^2}{2\kappa}C(\alpha)e^{-\kappa|x_2|}\right\}\sin(\alpha x_1)\,d\alpha\ ,$$

$$\beta_1=\frac{2Q_0c^2}{D(1-\nu^2)}\int_0^\infty\left\{\left[\left(\frac{(1-\nu)}{2}\alpha|x_2|-2\alpha^2\epsilon^2\right)A(\alpha)+\alpha B(\alpha)\right]e^{-\alpha|x_2|}+C(\alpha)e^{-\kappa|x_2|}\right\}\times\sin(\alpha x_1)\,d\alpha \tag{B11}$$

$$\beta_2=\frac{2Q_0c^2}{D(1-\nu^2)}\int_0^\infty\left\{\left[\left(\frac{(1-\nu)}{2}\alpha|x_2|-2\alpha^2\epsilon^2-\frac{(1-\nu)}{2}\right)A(\alpha)+\alpha B(\alpha)\right]e^{-\alpha|x_2|}+\frac{\alpha}{\kappa}C(\alpha)e^{-\kappa|x_2|}\right\}\cos(\alpha x_1)\,d\alpha \tag{B12}$$

$$Q_1=\frac{Q_0}{(1+\nu)}\frac{1}{\epsilon^2}\int_0^\infty\left\{-2\alpha^2\epsilon^2A(\alpha)e^{-\alpha|x_2|}+C(\alpha)e^{-\kappa|x_2|}\right\}\sin(\alpha x_1)\,d\alpha$$

$$Q_2 = \frac{Q_0}{(1+\nu)}\frac{1}{\epsilon^2}\int_0^\infty \left\{-2\alpha^2\epsilon^2 A(\alpha)\mathrm{e}^{-\alpha|x_2|} + \frac{\alpha}{\kappa}C(\alpha)\mathrm{e}^{-\kappa|x_2|}\right\}\cos(\alpha x_1)\,\mathrm{d}\alpha \ .$$

The solution must be finite at ∞ and satisfy the following boundary conditions:

$$\lim_{x_2\to 0^+} M_{22} = 0 \quad \forall x_1 \ , \tag{B13}$$

$$\lim_{x_2\to 0^+} M_{12} = 0 \quad \forall |x_1| < 1 \ , \tag{B14}$$

$$\lim_{x_2\to 0^+} Q_2 = -Q_0 \quad \forall |x_1| < 1 \ , \tag{B15}$$

$$\lim_{x_2\to 0^+} w = 0 \quad \forall |x_1| > 1 \ , \tag{B16}$$

$$\lim_{x_2\to 0^+} \beta_1 = 0 \quad \forall |x_1| > 1 \ . \tag{B17}$$

The substitution of the assumed forms into Eqs. (B9) and (B10) yields three coupled ODE's. With some work, they can be de-coupled resulting in sixth order equations that can be solved. Consistency can be used to reduce the number of unknowns to three. Then, Eq. (B13) can be used to reduce them to two. Employing the remaining boundary conditions, Eqs. (B14) through (B17) result in four integral equations. We then take a thick plate limit retaining only the largest terms. This results in two sets of decoupled dual integral equations

$$\frac{Q_0}{(1+\nu)}\int_0^\infty \left(\alpha(1+\nu) + \frac{\alpha}{\epsilon^2}\right)A(\alpha)\sin(\alpha x_1)\,\mathrm{d}\alpha = 0 \quad \forall |x_1| < 1 \ ,$$

$$\frac{2Q_0 c^2}{D(1-\nu^2)}\int_0^\infty A(\alpha)\sin(\alpha x_1)\,\mathrm{d}\alpha = 0 \quad \forall |x_1| > 1 \ .$$

and

$$\int_0^\infty \alpha B(\alpha)\cos(\alpha x_1)\,\mathrm{d}\alpha = (1+\nu)\epsilon^2 \quad \forall |x_1| < 1 \ ,$$

$$\int_0^\infty B(\alpha)\cos(\alpha x_1)\mathrm{d}\alpha = 0 \quad \forall |x_1| > 1 \ .$$

The solutions to these equations are

$$A(\alpha) = 0 \ , \tag{B18}$$

$$B(\alpha) = \frac{(1+\nu)\epsilon^2}{2}\frac{J_1}{\alpha} \ , \tag{B19}$$

$$C(\alpha) = \left(1 + 2\epsilon^2\alpha^2\right)A(\alpha) - \alpha B(\alpha) \ . \tag{B20}$$

yielding the solution

$$w(x_1,0) = \begin{cases} \frac{Q_0 c^3 \epsilon^2}{D(1-\nu)}\sqrt{1-{x_1}^2} & |x_1| < 1 \\ 0 & |x_1| > 1 \ . \end{cases}$$

References

1. **Abramowitz; Stegun:** Handbook of Mathematical Functions. Dover, New York 1965
2. **Belytschko, T.; Xiao, S.P.; Schatz, G.C.; Ruoff, R.S.:** Atomistic simulations of nanotube fracture. Phys Rev B 65 (2002) 235430–1/8
3. **Govindjess, S.; Sackman, J.L.:** On the use of continuum mechanics to estimate the properties of nanotubes. Solid State Commun 111 (1999) 227–230
4. **Hill, R.:** A self-consistent mechanics of composite materials. J Mech Phys Solids 13 (1965) 213–222
5. **Hill, R.:** Theory of mechanical properties of fibre-strengthened materials-iii: Self-consistent model. J Mech Phys Solids 13 (1965) 189–198
6. **Huang, M.; Suo, Z.; Ma, Q.:** Plastic ratcheting induced cracks in thin film structures. J Mech Phys Solids 50 (2002) 1079–1098
7. **Kachanov, M.:** Elastic solids with many cracks and related problems. In: Hutchinson, J.W.; Wu, T.Y. (eds) Advances in Applied Mechanics, pp. 259–445. New York. Academic Press 1994
8. **Knowles, J.K.; Wang, N.M.:** On the bending of an elastic plate containing a crack. J Math Phys 39 (1960) 223–236
9. **Lewinski, T.; Telega, J.J.:** Plates, Laminates and Shells: Asymptotic Analysis. Singapore, Eiver Edge NJ World Scientific 2000
10. **Li, S.:** The micromechanics of classical plates: A congruous estimate of overall elastic stiffness. Int J Solids Struct 37 (2000) 5599–5628
11. **Li, S.:** On micromechanics of reissner-mindlin plates. Acta Mech 142 (2000) 47–99
12. **Misawa, K.; Okabe, T.; Yanaka, M.; Shimizu, M.; Takeda, N.:** A theory of multi damage evaluation of tin thin film. Proceedings of the Material Research Society Symposium (2001) 653: Z7.10.1-Z7.10.6
13. **Naghdi, P.M.:** Foundation of elastic shell theory. In: Sneddon, I.N.; Hill, R.: (eds) Progress in Solid Mechanics. 4 Amsterdam North-Holland, 1963
14. **Naghdi, P.M.:** The theory of shells and plates. In: Flugge, S.; Truesdell, C. (eds) Handbuch. der Physik: Mechanics of Solids II, VI a/2. Berlin Springer Verlag, 1973
15. **Naghdi, P.M.; Rubin, M.B.:** Restrictions on nonlinear constitutive equations. J Elast 39 (1995) 133–163
16. **Nemat-Nasser, S.; Hori, M.:** Elastic solids with microdefects. In: Weng, G.J.; Taya, M.; Abe, H. (eds) Micromechanics and Inhomegeneity, pp. 297–320. New York Springer-Verlag, 1990
17. **Nemat-Nasser, S.; Hori, M.:** Micromechanics: overal. properties of heterogeneous materials. Amsterdam North-Holland, 1999
18. **Parton, V.Z.:** Engineering Mechanics of Composite Structures. Boca Raton, CRC Press, 1993
19. **Reddy, J.N.:** Mechanics of Laminated Composite Plates: Theory and Analysis. Boca Raton, CRS Press, 1997
20. **Reismann, H.:** Elastic Plates: Theory and Application. New York, John Wiley & Sons 1988
21. **Varias, A.G.; Mastorkos, I.; Aifantis, E.C.:** Numerical simulation of interface crack in thin films. Int J Fract 98 (1990) 195–207
22. **Wang, N.M.:** Effects of plate thickness on the bending of an elastic plate containing a crack. J Math Phys 47 (1968) 371–390
23. **Wang, N.M.:** Twisting of an elastic plate containing a crack. Int J Fract Mech 6 (1970) 367–378
24. **Young, M.J.; Sun, C.T.:** Cracked plates subjected to out-of-plane tearing loads. Int J Fract 60 (1993) 1–18